Multiparametric MRI and Ultrasound in the Preoperative Assessment of Borderline Versus Malignant Ovarian Tumors

Ayatullah Gharib Mostafa[1,5], Fatma Mohamed Awad[1,] Ahmed Abd El Karim Abd EL Salam Fayed[1], Hassan Mostafa Gaafar[2,3], Tarek M. Zaghloul[2,4], Yasmin Essam Khalifa[1], Soha Talaat Hamed[1]

[1] Department of Radiodiagnosis, Kasr El Aini, Cairo University Hospitals, Cairo, Egypt.
[2] Department of Surgical Oncology, National Cancer Institute, Cairo University, Egypt.
[3] Department of Gynecology & Obstetrics, Kasr El Aini, Cairo University Hospitals, Cairo, Egypt.
[4] Department of Surgery, St. Jude Children's Research Hospital, TN, USA.
[5] Department of Diagnostic Imaging, St. Jude Children's Research Hospital, TN, USA.
Corresponding Author: Ayatullah G. Mostafa
Email: ayagharibmostafa@gmail.com

Abstract

Background: Characterization of borderline ovarian lesion represents a diagnostic challenge; it is of great importance in the preoperative assessment to plan adequate therapeutic procedures, especially in women in the childbearing period aiming to preserve fertility. Objective: to evaluate the utility of ultrasound, Doppler, and multiparametric MRI in the assessment of borderline ovarian masses. As well as the detection of different significant diagnostic criteria in differentiating borderline from malignant ovarian masses. Methods: The study included 72 ovarian masses in 68 patients. Their final pathological results were 29 borderline and 43 malignant lesions. All patients underwent preoperative ultrasound, Doppler and contrast-enhanced MRI, and images were retrospectively reviewed and compared between the 2 pathologies. Results: Borderline ovarian masses were significantly more observed in younger pre-menopausal women compared to their malignant counterparts. No significant difference was noted in CA-125 level between both patient groups. In this study, we identified eight significant imaging features that can be used to differentiate borderline from malignant ovarian masses: maximum lesion diameter, lesion shape, number of papillary projections/solid parts, size of the largest solid part, cystic-solid interface, ovarian crescent sign, and ascites. No significant difference was found in the size of the septations, site and degree of vascularity, resistivity index, the pattern of post-contrast enhancement, or diffusion/apparent diffusion coefficient. Conclusion: Imaging findings of these 2 pathologies overlapped considerably. Compared with BOTs, MOTs exhibited larger tumor size, irregular shape, larger solid parts, lower RI, unclear solid cystic interface, effaced ovarian tissue, and a larger amount of ascites. A combination of clinical data including age, and menopausal status with different imaging criteria can improve the diagnostic performance.

Keywords: ultrasound, Doppler, MRI, borderline ovarian lesions, malignant ovarian lesions.

1. Introduction

Ovarian cancer was the third most common gynecological cancer globally in 2020 and is one of the highest incidences of cancer-related deaths of all female reproductive systems (1). There are two pathways for the development of ovarian neoplasms. The first follows a stepwise pathway from a benign tumor (i.e., cystadenoma) to a borderline tumor and finally to a malignant tumor. The second pathway lacks the presence of a pre-invasive lesion and directly becomes malignant (2). Ovarian Borderline tumors are a unique pathologic subtype of ovarian epithelial tumors that comprise 14-20% of primary ovarian neoplasms. They are characterized by their low malignant potential and nuclear atypia with no stromal invasion (3). The mean age of occurrence is approximately 10 years younger than that of women with frankly malignant ovarian cancer. Consistently, they have a better prognosis than their malignant counterparts, which is related to their carcinogenetic pathway and biological behavior. The reported 5-year survival rate is 92%, in contrast to 35% for MEOT (2,4).

Because a high proportion of women with BOTs are young and the prognosis is excellent, early diagnosis is crucial as well as preoperative identification of those patients can guide the surgeon to consider fertility-sparing procedures, avoiding unnecessary excision of the ovary and uterus, and improving the patient's postoperative quality of life (5). Approximately 23% of patients remain asymptomatic at the time of diagnosis; thus, the tumors are incidentally found (6). When symptomatic, clinical signs and symptoms are often vague and present

doi.org/10.31838/hiv23.03.134 Received: 07.11.22, Revised: 19.12.22, Accepted: 24.01.23.

late in the course of the disease in the form of abdominal pain and distension (7).

US is the first-line imaging modality for adnexal lesions and is a particularly useful preoperative test for the characterization of adnexal masses, having an enhanced ability to detect subtle morphologic changes in the ovaries (8). Magnetic resonance imaging (MRI) may be of great help in identifying complex lesions before surgery, particularly when US findings are suboptimal or indeterminate (9). MR imaging can also help determine additional diagnostic information, such as the presence of fat, blood products, solid components, peritoneal implants, fibrosis, and enhancement pattern or diffusion restriction (10). In this study, we combined both imaging tools to detect the utility of different imaging parameters to differentiate between borderline and malignant ovarian neoplasms.

2. Materials and methods

2.1. Patients:

Our institution's institutional review board approved this retrospective study and written informed consent was waived. A series of 121 histopathologically proven ovarian neoplasms were diagnosed using surgical specimens at our institution from October 2018 to October 2022. We excluded 49 ovarian lesions because they either had no preoperative MRI (n = 33) or no ultrasound (n = 16) (Fig. 1). We had 10 out of the 49 excluded lesions having solid components in more than 80% of the lesion and were defined as solid tumors proved pathologically to be malignant lesions. The remaining 72 ovarian lesions (in 68 patients) constituted the study population. They included 29 borderline lesions in 29 patients (age range, 21–78; mean age, 46.6 ± 15.1 years) and 43 malignant lesions in 39 patients (four patients had bilateral malignant lesions) (age range, 31–81; mean age, 55.3 ± 17.9 years). The included patients' preoperative ultrasound, Doppler, and MRI images were evaluated retrospectively. The serum levels of CA 125 were measured in all patients preoperatively using the CA 125 II immunoradiometric assay, and the results were expressed in U/mL with a cut-off value of 35 U/ml.

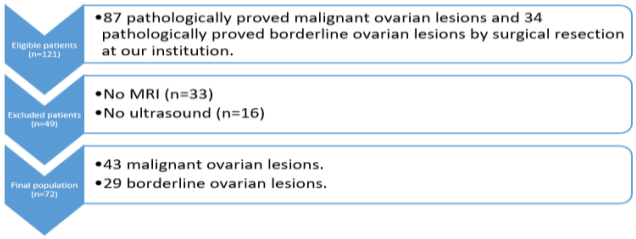

Fig. 1. Flow diagram of the study enrollment population.

2.2 Imaging protocol

The patients were referred from the Gynecology Department to the Radiology Department (Women's Imaging Unit) during the period from October 2018 to October 2022. All patients were counseled and signed a consent form. All the patients were investigated for renal function (serum creatinine, urea level, and urine analysis). All included patients undergone ultrasound, Doppler, and contrast-enhanced MR imaging. Image assessment was independently reviewed by 2 radiologists with 7 and 21 years of post-training experience in gynecological imaging. Any disagreements between the radiologists were resolved by consensus. Ultrasound examination was done on an ultrasound machine GE logic 7, trans-abdominal and trans-vaginal ultrasound approaches were done using 3-4 MHz and 7-8 MHz probes respectively. A general assessment of the female pelvic organs (uterus, bladder, Douglas pouch, and adnexa) was done prior to the targeted lesion and ovaries detailed assessment. The masses were described using the terms and definitions of the IOTA group 22 (11).

Ovarian lesions were classified as unilocular solid, multilocular, and multilocular solid according to previously reported classification for adnexal masses by (12). In the presence of intralesional solid tissue, the ovarian mass was described as unilocular-solid or multilocular-solid, depending on whether a single cystic locule or multiple locules were found. If the solid tissue appeared as an echogenic structure projecting within the cystic component, this was defined as 'papilla'. The International Ovarian Tumor Analysis group recommends that all papillary projections should be recorded as a solid component (11). The number and size of the papillary projections were assessed, as well as the presence of septae and their thickness. The ovarian crescent sign was defined as visible hypoechoic tissue, with or without ovarian follicle, located adjacent to the cyst wall.

All color Doppler examinations began with the same settings of the ultrasound system: the highest sensitivity for detection of color Doppler signals was used allowing detection of blood flow velocities ≥3 cm/s, and the color gain was set just below the background noise level to increase, as far as possible, the Doppler sensitivity for low velocity flow detection. A subjective semiquantitative assessment of the amount of blood flow within the examined tumor was made (color score): a score of 2 was given when mild color could be detected, a score of 3 was given when a moderate amount of color was present, and a score of 4 was given when the tumor appeared highly vascular. Site of vascularity is also recorded; being peripheral or central, within the septations, papillary or solid parts. The color Doppler sensitivity was reduced by increasing the pulse repetition frequency until only one vessel was detectable. Pulsed Doppler examination of this vessel enabled spectral analysis of the blood flow. The resistivity index (RI) was recorded. Photographic images were printed, and ultrasound digital images were stored on a hard disk for subsequent review and analysis.

MR imaging was performed using a 1.5 T MR imaging system (Intera Achieva 1.5 T Pulsar; Philips Medical Systems, Best, The Netherlands) or a 3 T MR

imaging system (Intera Achieva 3.0 T Quasar Dual; Philips Medical Systems, Best, The Netherlands). Patients were imaged in the supine position with the aid of pelvic phased-array coil. All patients should be fasting for 3 h and voiding urine 2 h prior to examination. Conventional MRI T1 and T2 WI were taken. DW-MRI was done in the axial plane using a single-shot echo-planar imaging sequence at different b values. Diffusion and ADC value were assessed. In case of numerous vegetations, papillary projections, or thickened septa, ROIs were drawn within the targeted components and the mean ADC value was used in the analysis. DCE-MRI was done in all patients, and post-contrast T1 fat sat THRIVE images were obtained immediately after being injected with gadolinium at a dose of 0.1 mmol/kg of body weight (maximum, 20 mL), then ROI size varied from 15 to 150 mm2 put on the targeted area then one the three dynamic curve types is recorded.

2.3. Statistical analysis

IBM® SPSS® v28 was used for data analysis. Qualitative data is presented as frequency and relative frequency while the quantitative data is presented as mean and standard deviation. Data were checked for distribution of normality; then using independent sample t-test or Mann Whitney U test and Chi-squared test or Fisher's exact test to test the statistical-significance difference between BOT and malignant groups as regards various criteria. ROC curve and AUC were used to know the cut-off value of the size of solid/papillae to distinguish/predict the BOT and malignant tumors.

3. 3.Results

This study included 72 ovarian lesions in 68 patients. Bilateral malignant lesions were noted in 4 patients. The age of BOT patients ranged from 23 to 55 years with mean ± SD (41.31 ±7.48 years), while the age of patients with malignant ovarian tumors ranged from 37 to 72 years with mean ± SD (56.47 ±8.96 years) with a statistically significant difference in age among both groups. Menopausal status was significantly observed among the malignant group (30 patients, 69.8%) while only four patients (13.8%) among the BOT group were post-menopausal females. A statistically significant relation between menopause and type of tumor; p-value <0.001, OR (95% CI) = 14.4 (4.2-49.8) was noted.CA-125 was measured in all study patients being >35 U/ml in 17 patients (58.6%) with BOT and 30 patients (68.9%) with malignant lesions with no significant difference detected. Pathological subtypes of both groups are shown in table 1.

Table 1: Pathological classification of borderline and malignant lesions.

	Pathological type	Frequency	Relative frequency (%)
Borderline	Serous	18	62
	Mucinous	10	35
	Endometrioid	1	3
Malignant	Serous adenocarcinoma	24	56
	Mucinous adenocarcinoma	10	23
	Clear cell carcinoma	4	9
	Endometroid carcinoma	2	5
	Malignant granulosa cell tumor	2	5
	Malignant brenner tumor	1	2

Tumor characteristics detected by both imaging tools are shown in table 2. There is a statistically significant difference of 4.7cm (95% CI: 1.2,2.2) between both groups regarding the tumor's maximum diameter. Lesion shape, solid/cystic interface, number of papillary projections, size of the largest solid part, and the presence or absence of ascites were found to be a statistically significant factors to differentiate between both groups.

Table 2: Tumor characteristics detected by both MRI and US per pathological group.

		BOT(N=29)	Malignant(N=43)	P-value	OR (95% CI)
Max Diameter(cm); Mean (±SD)		10.34 ±5.86	15.02 ±4.62	<0.001	4.7(1.2-2.2)*
Shape	Regular	27 (93.1)	26 (60.5)	0.002	8.8 (1.85-42.04)
	Lobular/irregular	2 (6.9)	17 (39.5)		
Lesion character	unilocular with papillae /nodule /solid part	12 (41.4)	22 (51.2)	0.372	
	Multilocular	6 (20.7)	4 (9.3)		
	Multilocular solid	11 (37.9)	17 (39.5)		
Cystic solid interface	clear	29 (100)	17 (39.5)	<0.001	
	unclear	0	26 (60.5)		
Ascites	No	22 (75.9)	11 (25.6)	<0.001	9.1 (3.1-27.3)
	Yes	7 (24.1)	32 (74.4)		
size of septa (n=36)	≤ 5 mm	9 (60)	6 (28.6)	0.059	3.8 (0.9-15.2)
	> 5 mm	6 (40)	15 (71.4)		
Number of papillae (n=61)	≤ 3	12 (54.5)	5 (12.8)	<0.001	8.2 (2.3-28.7)
	> 3	10 (45.5)	34 (87.2)		
size of the largest solid part (n=61)	< 3 cm	19 (86.4)	11 (28.2)	<0.001	16.1 (4-65.6)
	≥ 3 cm	3 (13.6)	28 (71.8)		
Size of largest solid/papillae (in mm): mean (± SD)		20.2(±12.7)	34.5(±11.6)	<0.001	14.3 (7.9-20.9)*

*mean difference (95% CI)

The ROC curve analysis for the maximum tumor diameter (Fig 2 a) yielded a cut-off score of 10.5cm with an area under the curve (AUC) of 0.711, a sensitivity of 86%, and a specificity of 69% for distinguishing BEOTs from MEOTs. Another curve (Fig 2b) was also done for the size of the largest solid part; yielded a cut-off score of 24mm with an area

under the curve (AUC) of 0.812, a sensitivity of 79.5%, specificity of 72.7% for distinguishing BEOTs from MEOTs.

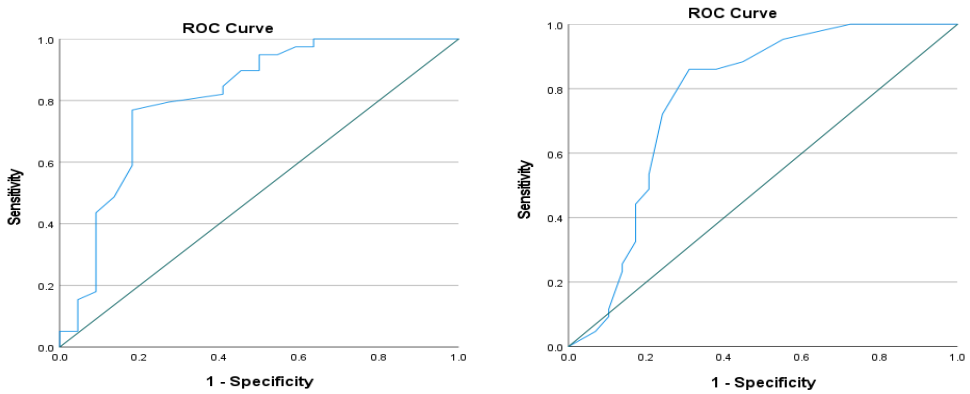

Fig. 2. The receiver-operating characteristic curves of a) The right curve showing the size of the largest solid part, b) The left curve showing the maximum tumor diameter.

Specific ultrasound, Doppler, and MRI criteria among both groups are shown in Tables 3 &4. Resistivity index was significantly lower in malignant compared to borderline ovarian masses. ADC value ranged from 0.65 to 1.50 × 10−3 mm2/s with a mean of 0.72x10−3 mm2/s (±0.23) and ranged from 0.52 to 1.25 × 10−3 mm2/s with a mean of 0.68x10−3 mm2/s (±0.24) for borderline and malignant cases respectively, with no significant statistical difference noted.

Table 4: US findings per pathological group.					
		BOT (N=29)	Malignant (N=43)	P-value	OR (95% CI)
Ipsilateral crescent sign	Present	19 (65.5)	3 (7)	<0.001	
	Absent	10 (34.5)	40 (93)		
Arrangement of vessels	Peripheral	4 (13.8)	6 (14)	>0.999	0.99 (0.25-3.9)
	Central	25 (86.2)	37		
Degree of Vascularity	Mild	1 (3.4)	0	0.137	
	Moderate	19 (65.5)	21 (48.8)		
	Marked	9 (31)	22 (51.2)		
Site of vascularity	Solid/ Papillae	13 (44.8)	25 (58.1)	0.33	
	Septal	6 (20.7)	4 (9.3)		
	Both	10 (34.5)	14 (32.6)		
RI (resistivity index)	> 0.4	18 (62.1)	12 (27.9)	**0.004**	
	≤ 0.4	11 (37.9)	31 (72.1)		

Table 5: Dynamic curve types and DWI signal per pathological group.				
		BOT (N=29)	Malignant (N=43)	P-value
Dynamic curve type	type 1 curve	1 (3.4)	0	0.073
	type 2 curve	17 (58.6)	16 (37.2)	
	type 3 curve	11 (37.9)	27 (62.8)	
DWI (diffusion)	Facilitated DWI	9 (31)	11 (25.6)	0.612
	Restricted DWI	20 (69)	32 (74.4)	

Fig 3.

a- **b-**

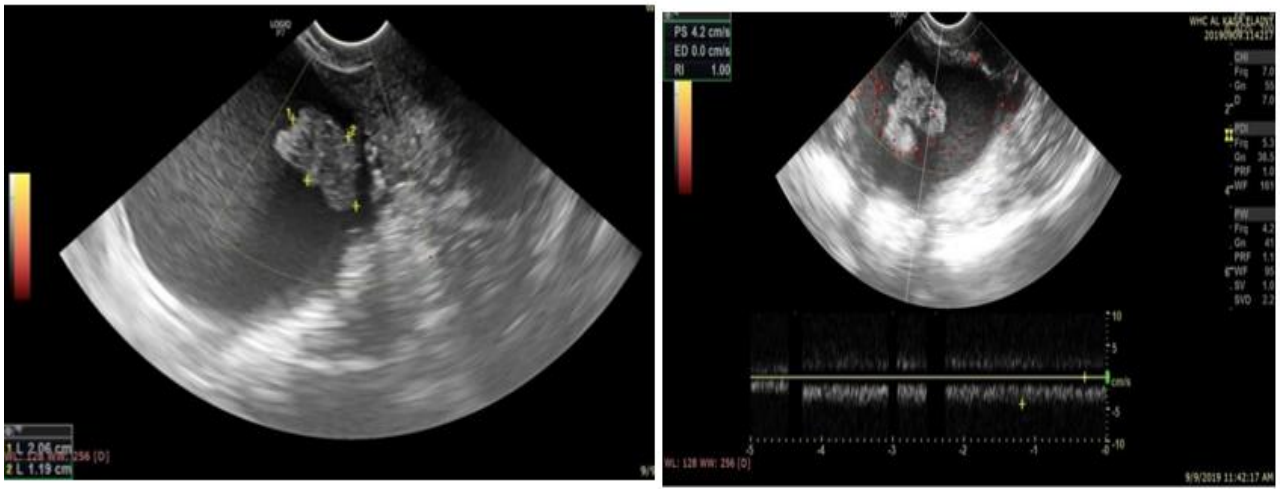

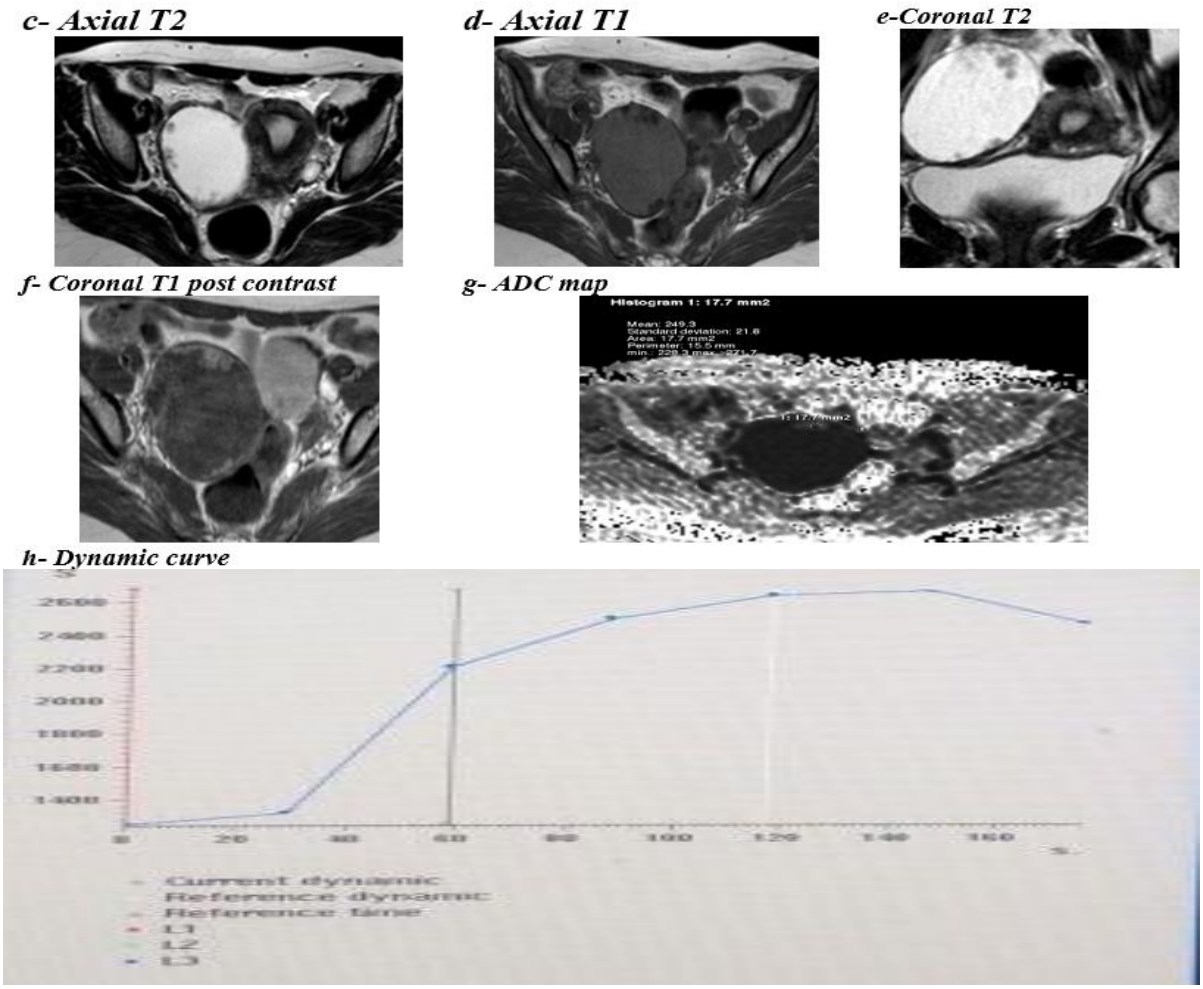

Figure 3: A 47-year-old female presented with an accidentally discovered adnexal lesion during an ultrasound exam for another cause. CA-125 was elevated (63U/ml). (a-b) Ultrasound images show a right adnexal unilocular cystic lesion measuring 7 cm with internal papillary projections, the largest measuring 2 cm. By color Doppler examination, mild vascularity within the solid part was observed with color score 2 and RI=1. Conventional MRI: (c-e) axial T2, axial T1, and coronal T2 weighted images show a right adnexal unilocular cystic lesion measuring 9 cm with internal papillary projections that elicit iso-intense T1 and high T2 signals. (f) Post-contrast axial T1 WI shows intense post-contrast enhancement of its papillary projections. (g) Diffusion WIs and ADC map: demonstrate diffusion restriction of the mural nodules. ADC value measures 0.24 x10-3mm2/S. (h) DCE: DCE shows type I curve: continuously rising curve. Final pathological diagnosis (post right oophorectomy): Right serous borderline ovarian tumor.

Fig4:

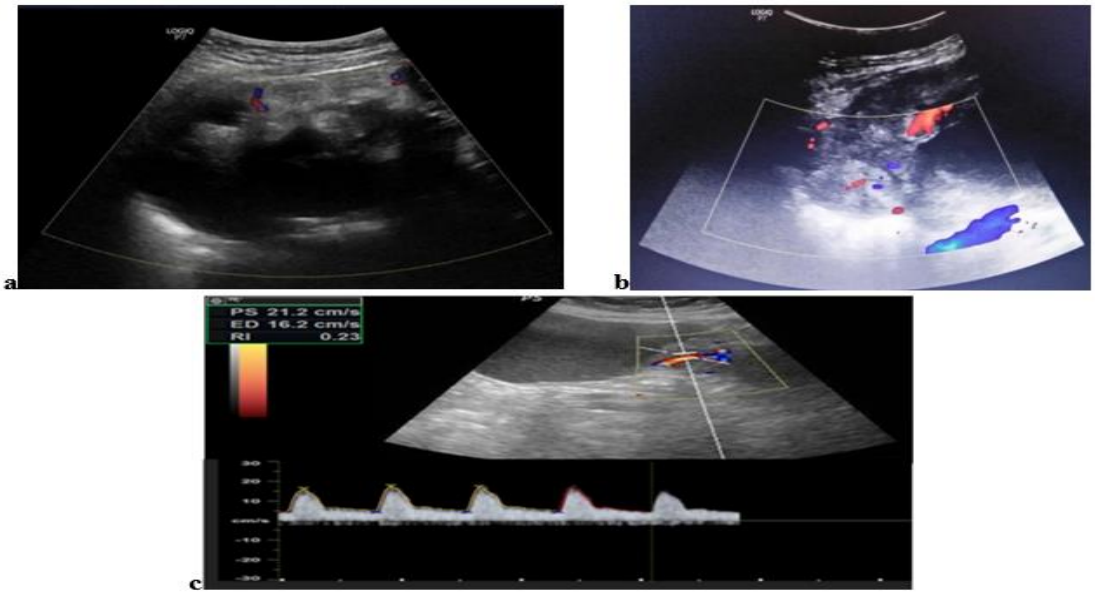

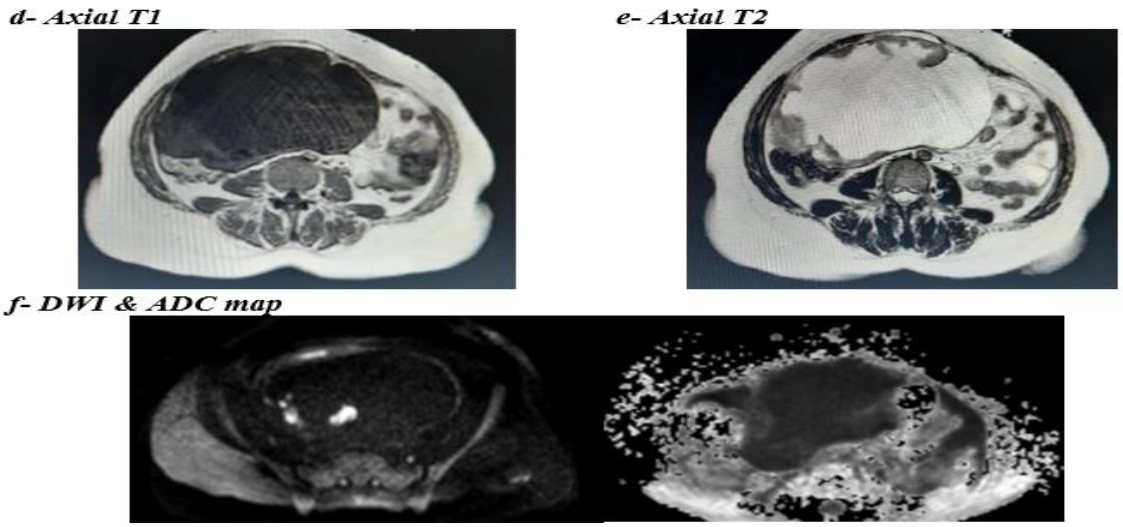

Fig 4: A 38-year-old female presented with menstrual irregularities with pelvic discomfort. CA-125 was elevated (180 U/ml). Ultrasound images show (a&b) right unilocular cystic adnexal lesion with endophytic papillary projections and thickened mural nodules measuring 17 cm, the largest solid part measuring 40mm showing vascularity within with color score 3. (C) RI within the vascular part =0.23. (d-f) Conventional MRI: (d,e) axial T1 and T2 weighted images show a large right adnexal unilocular cystic lesion it measures 17cm with endophytic papillary projections and thickened mural nodules reaching 4 cm in diameter. The solid parts elicit intermediate T1 and T2 signals. (f)Diffusion WIs and ADC map: show diffusion restriction the some of the solid parts with an estimated ADC value of 0.6 x10-3mm2/S. (g) Post-contrast axial T1: demonstrates intense post-contrast enhancement of the solid parts. Arrows showing the enhancing solid parts (h) DCE: type III curve: initial rapid rise with early washout. Final pathological diagnosis (post total abdominal hysterectomy): Right ovarian serous adenocarcinoma.

Fig 5

a-

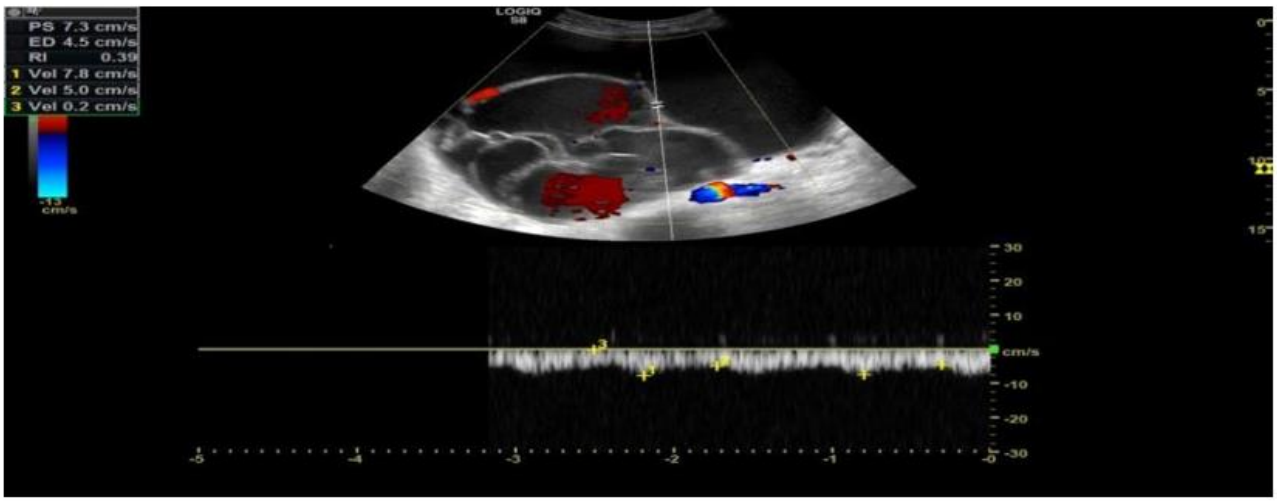

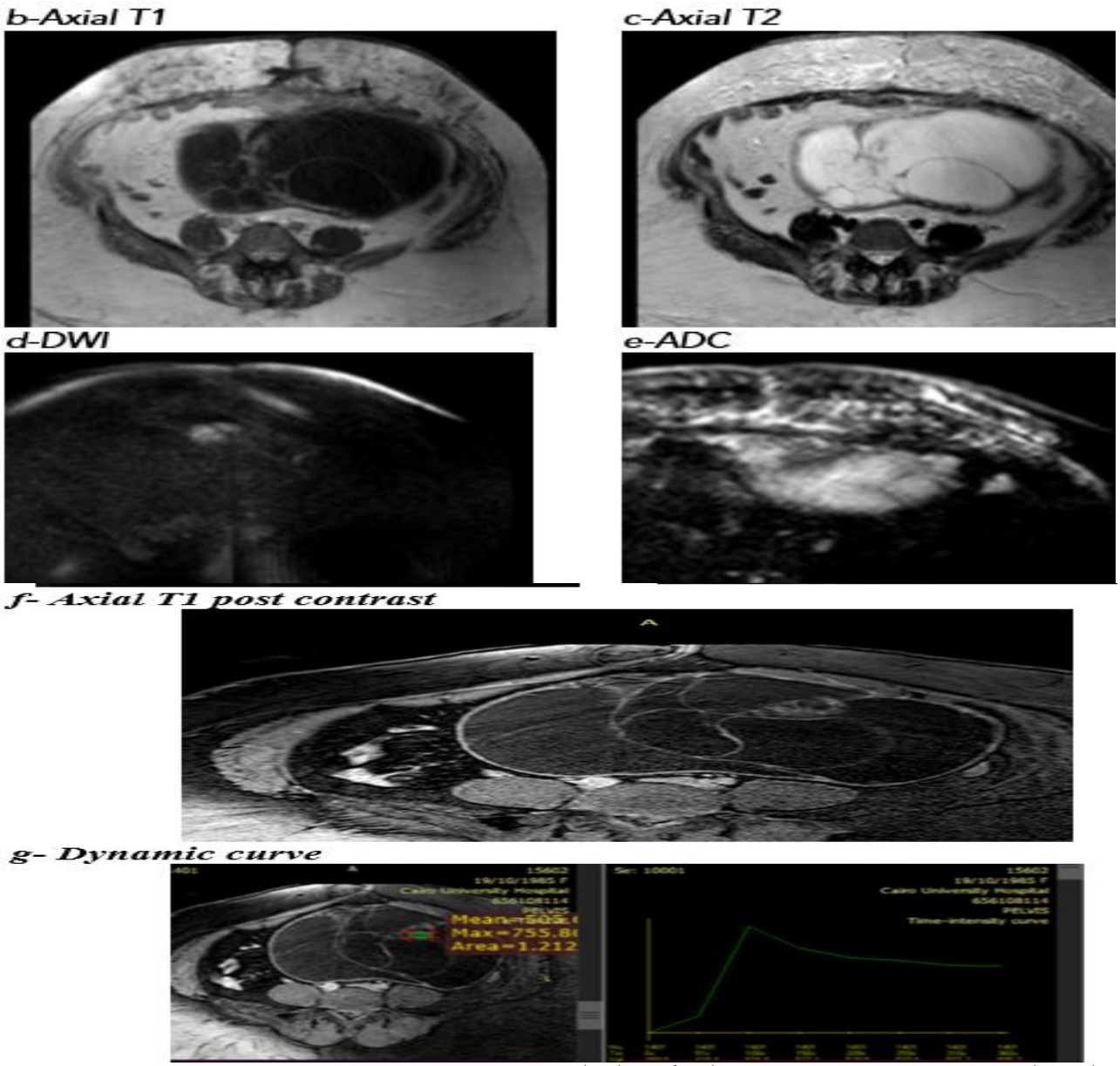

Figure 5: (a): Ultrasound images show a left multilocular solid cystic lesion with internal thick internal septations (reaching 6 mm). Color Doppler study revealed vascularity within the septations with color score 3 and RI=0.39. **Conventional MRI: (b,c)** axial T1 and T2 weighted images show a left pelviabdominal multilocular cystic adnexal lesion measuring 13 cm with multiple internal septations eliciting intermediate T1 and low T2 signal. **(d&e) DWI** show diffusion restriction of part of the honeycomb nodule. **(f) Post-contrast** axial and coronal T1 images show avid enhancement of the internal septations **(g) DCE** shows a type III curve: initial rapid rise followed by a rapid washout. **Final pathological diagnosis** (post left oophorectomy): Left mucinous borderline ovarian tumor.

4. Discussion

Preoperative characterization of an ovarian lesion carries great importance to plan adequate therapeutic procedures, especially in premenopausal women because of the desirability of preserving ovarian function and fertility with less radical fertility-sparing surgery (unilateral oophorectomy or cystectomy) recommended in those patients. In contrast, surgical management of stage I epithelial ovarian carcinoma (EOC) is completely different, as necessary complete staging requires pelvic and paraaortic lymph node dissection (13).

It has been clearly established in several studies that these tumors occur in patients who are younger compared with those who develop invasive carcinomas and they have been reported to exhibit a relatively benign clinical course with a more favorable prognosis (4,14,15).

The present study showed a significant difference between the pathology of the lesion in relation to the age and menopausal state which was also encountered in previous studies as most of the borderline cases are diagnosed in pre-menopausal women between 30 and 40 years, while malignant ovarian cancer usually is diagnosed in post-menopausal women between 50 and 70 years (13,16,17).

CA-125 was measured in all the study patients with no significant difference among both groups; this

was in accordance with Souza et al, 2005 who found that CA-125 has been normal or marginally raised in BOTs while Lee et al, 2011 suggested an additional role for CA-125 overlapping radiological findings for differentiation of BOTs from stage I carcinoma, and found that CA-125 levels for solid components and thick septations are significantly higher in stage I carcinoma than in BOTs (18,19). Serum CA 125 can be elevated in BOT patients, but it should not be used to predict the nature and invasiveness of the tumor (20,21).

Among ovarian borderline tumors, approximately 70 % are serous histology, while mucinous BOTs are less common than their serous counterparts. They are also called "atypical proliferative mucinous tumors" (APMT) or "mucinous tumors of low malignant potential" (22). In our study, we had 62% serous, 35% mucinous, and 3% endometroid BOT. The latter consists of atypical endometroid cells lacking destructive stromal invasion. This study identified eight significant imaging features of BEOTs; lesion size, shape, number of papillary projections/solid parts, size of the largest solid part, cystic-solid interface, ovarian crescent sign, ascites, and RI.

Previous studies classified BEOTs (23,24): as purely cystic; predominantly cystic with papillary projections or solid parts; and solid. In this study, purely cystic was not observed in the BEOTs, while predominantly cystic with papillae, mural nodules or solid parts was the most frequent pattern recorded (79%) which is congruent with previous studies (13,23,25). Papillary growth pattern with internal branching, also known as sea anemone-like appearance, is a specific MR picture of BEOTs (24,26). They frequently appeared regular in shape with well-defined margins and clear cystic-solid interfaces. In contrast, MEOTs often had a lobulated or irregular shape, ill-defined margins, and unclear cystic-solid interfaces. The aforementioned criteria were significantly observed in our study.

In contrast with women with ovarian carcinoma, those with borderline tumors (BOTs) are unlikely to present with ascites, bowel obstruction, pleural effusion, or venous thromboembolism (27,28,29). Moderate or marked ascites were found in 24% of BEOTs and 74.4% of MEOTs, a significant difference that could be used as a factor to determine the nature of the tumor, but a previous study suggested that ascites cannot effectively distinguish borderline from malignant ovarian tumors (30). The mean size of the borderline lesions was 10.3 cm which is smaller than the malignant lesions mean size (15 cm), being consistent with those previously detected in other studies (17,29).

Thick septations >5mm were observed in both patient groups with no considerable difference which was congruent with the quantitative and qualitative results of Kaga et al, 2020. Seven false positive cases were diagnosed as BOTs by imaging and pathologically proved benign had thick internal septations which were found not to be a significant factor to depend on in this study. One of these seven cases was pathologically proven cystic adenofibroma, accounting for about 1.7% of all benign ovarian tumors (31). Cystic adenofibroma may mimic malignant neoplasm on imaging as well as on intraoperative findings (32). The size of the largest solid part among the BOT was significantly smaller than their malignant counterparts as shown in other studies (13,29,33), we calculated an optimal cut-off value of 24mm. Kaga et al, 2020 reported a lower optimal cut-off value of 19 mm when comparing mural nodules in mucinous carcinomas (MCs) with mucinous BEOTs, but they also concluded that the size of mural nodules is a significantly important factor to distinguish MCs from mucinous BEOTs. The number of papillary projections was significantly higher in the malignant compared to borderline cases. Papillary projections of more than 3 in number were only observed in 45.5% of the borderline cases while in 87.2% of the malignant cases. This observation was also recorded in Moro et al, 2017 study who found papillary projections >3 in all malignant cases and only 33% of the borderline cases (34).

The ovarian crescent sign was defined as visible hypoechogenic tissue with or without ovarian follicles enclosed within the ovarian capsule encircling the tumor and located adjacent to the cyst wall. This tissue would not be separated from the cyst when applying a moderate amount of pressure (35). While often distorted, an ipsilateral normal ovary was found in 7% of MEOTs in our study because they infiltrate and destroy the ovarian structure, while ipsilateral ovary could be detected in about 65% of the borderline cases. So, we concluded that presence of ovarian crescent sign makes diagnosis of malignant lesion very unlikely.

Color Doppler examinations indicate that a low resistance, similar to invasive ovarian cancers, may characterize vascular flow within borderline tumors. In this study, RI (resistivity index) was noted to be significantly lower in malignant lesions. RI equal to or less than 0.4 was noted in 72.1% of the malignant cases, and in 37.9% of borderline cases, with a P-value=0.004. A previous study stated that measurement of RI in BOT's yielded values intermediate between those of benign tumors and ovarian cancers with gradual lowering, but these differences were not statistically significant (36). However, these observations have not been confirmed in all studies, and reliable differentiation by color Doppler examination of vascular flow is not possible, as RI values may show significant overlap between borderline and malignant tumors (25,37,). In Sobiczewski et al, 2012 study, mean RI values in ovarian cancers and borderline ovarian tumors were 0.48 and 0.51, respectively (17).

Central vascularity was noted in about 86% of the malignant as well as borderline lesions. The degree of vascularity by ultrasound as well as post-contrast enhancement criteria by MRI and dynamic curves did not show any considerable difference among both groups. Steady rise curve (Type 2 curve) and

enhancement then rapid wash out curve (Type 3 curve) are the usual curve patterns detected in both groups. There was overlap among the curve types of the malignant and borderline lesions; therefore, their capacity to differentiate borderline from malignant tumors was low, as stated in many previous studies (38,39,40). Although DCE-MRI has high specificity for depicting invasive lesions, DCE-MRI techniques are also prone to pitfalls. False-negative results may occur with poorly vascularized malignant tumors, and false-positive enhancement characteristics may be seen in benign lesions with a high blood supply, such as tubo-ovarian abscess, which may appear complex and indeterminate with all imaging modalities (41).

In this study DWI and ADC measurement in the solid components or thickened septations was not found to be a tool for differentiating borderline from malignant lesions. ADC mean value was 0.72x10−3 mm2/s (±0.23) and 0.68x10−3 mm2/s (±0.24) for borderline and malignant cases respectively.

When diffusion restrictions or small ADC values are detected, this may indicate a malignant tissue or the presence of hypercellularity. Results in the literature regarding the utility of DWI and ADC in discriminating benign, borderline, and malignant adnexal lesions have been conflicting and it may be occasionally difficult to differentiate (42,43,44). There are several studies that analyzed the ADC values of ovarian tumors. On the basis of these results, the ADC values of borderline epithelial ovarian tumors ranged from 1.62 to 1.70 × 10−3 mm2/s and those of malignant epithelial ovarian tumors ranged from 0.87 to 1.25 × 10−3 mm2/s (45,46). Kawaguchi et al, 2020 study detected a significantly lower ADC value in low-grade serous carcinomas compared to serous BOT's.

This study was limited by the small sample size in relation to multiple imaging parameters. It is well known that retrospective studies are more prone to biases. It is difficult or even impossible to eliminate them completely and, in the process of attempting to do so, new biases may be introduced.

5. Conclusion

Accurate diagnosis of BOT's is very challenging, as imaging findings of these 2 pathologies overlapped considerably. A combination of variable ultrasound, Doppler, and MRI parameters can improve the diagnostic performance of differentiating borderline from malignant lesions. As well as the combination of clinical data such as age, menopausal status, and CA125 level to imaging criteria can be helpful in suggesting a BOT rather than other pathology. Compared with BOTs, MOTs exhibited larger tumor size, irregular shape, larger solid parts, lower RI, unclear solid cystic interface, with effaced ovarian tissue, and a larger amount of ascites

6. Disclosure

Drs. Ayatullah Gharib Mostafa, Fatma Mohamed Awad, Ahmed Abd El Karim, Hassam Mostafa Gaafar, Tarek M. Zaghloul, Yasmin Essam Khalifa, and Soha Talaat have no conflicts of interest or financial ties to disclose

Ethical disclosure

The authors state that they have obtained appropriate institutional review board approval. Informed consent has been obtained from all the participants involved.

Abbreviations

BOT: Borderline ovarian tumors
MOT: malignant ovarian tumors
MRI: magnetic resonance imaging
US: ultrasound
RI: resistivity index
DWI: diffusion-weighted imaging
ADC: apparent diffusion coefficient
IOTA: The International Ovarian Tumor Analysis

References

Sung H., Ferlay J., Siegel R.L., Laversanne M., Soerjomataram I., Jemal A., Bray F. Global Cancer Statistics 2020: GLOBOCAN Estimates of Incidence and Mortality Worldwide for 36 Cancers in 185 Countries. *CA A Cancer J. Clin*. 2021;71:209–249.

Fischerova D, Zikan M, Dundr P, Cibula D. Diagnosis, treatment, and follow-up of borderline ovarian tumors. Oncologist. 2012;17(12):1515-33. doi: 10.1634/theoncologist.2012-0139. Epub 2012 Sep 28. PMID: 23024155; PMCID: PMC3528384.

Naqvi J, Nagaraju E, Ahmad S. MRI appearances of pure epithelial papillary serous borderline ovarian tumours. Clin Radiol 2015; 70:424–432.

Bouic-Pagès E, Perrochia H, Mérigeaud S, et al. MR imaging of primary ovarian tumors with pathologic correlation, J. Radiol. 2009; 90: 787–802.

Uzan C, Muller E, Kane A, Rey A, Gouy S, Bendiffallah S, Duvillard P, Fauvet R, Darai E, Morice P. Prognostic factors for recurrence after conservative treatment in a series of 119 patients with stage I serous borderline tumors of the ovary. Ann Oncol. 2014 Jan;25(1):166-71. doi: 10.1093/annonc/mdt430. Epub 2013 Nov 28. PMID: 24287939.

Skirinisdotti I. Borderline Ovarian tumors in Sweden 1960-2005: trends in incidence and age at diagnosis compared to ovarian cancer. Int J Cancer 2008; 123(8): 1

Torre LA, Trabert B, DeSantis CE, Miller KD, Samimi G, Runowicz CD, Gaudet MM, Jemal A, Siegel RL. Ovarian cancer statistics, 2018. CA Cancer J Clin. 2018 Jul;68(4):284-296. doi: 10.3322/caac.21456. Epub 2018 May 29. PMID: 29809280; PMCID: PMC6621554.

Tajada-Bergés T, Trimble EL, Shetty MK, Ovarian Cancer Screening and Early Detection in Low and Middle-Income Countries, Breast and Gynecological Cancers 2013; 125-148.

Zhang P, Li W, Chu C, Cui Y and Zhu M. Diffusion-weighted MRI: a useful technique to discriminate benign versus malignant ovarian surface epithelial

tumors with solid and cystic components 2012; 37: 897-903.

Halankar, Jaydeep, Glen Lo, and Ur Metser. "MRI classification and characterization of complex ovarian masses." Appl Radiol 46, no. 3 (2017): 6-20.

Timmerman D, Valentin L, Bourne TH, Collins WP, Verrelst H, Vergote I. Terms, definitions and measurements to describe the sonographic features of adnexal tumors: a consensus opinion from the International Ovarian Tumor Analysis (IOTA) Group. Ultrasound Obstet Gynecol. 2000;16:500–5

Timmerman D, Van Calster B, Testa A, Savelli L, et al. Predicting the risk of malignancy in adnexal masses based on the Simple Rules from the International Ovarian Tumor Analysis group. American journal of obstetrics and gynecology. 2016 Apr 1;214(4):424-37.

Zacharakis D, Thomakos N, Biliatis I, Rodolakis A, Simou M, Daskalakis G, Bamias A, Antsaklis A. Ultrasonographic markers and preoperative CA-125 to distinguish between borderline ovarian tumors and stage I ovarian cancer. Acta obstetricia et gynecologica Scandinavica. 2013 Mar;92(3):285-92.

Camatte S, Morice P, Thoury A, Fourchotte V, Pautier P, Lhomme C, Duvillard P, Castaigne D. Impact of surgical staging in patients with macroscopic "stage I" ovarian borderline tumours: analysis of a continuous series of 101 cases. European Journal of Cancer. 2004 Aug 1;40(12):1842-9.

Fauvet, Raffaèle, Christophe Poncelet, Joëlle Boccara, Philippe Descamps, Eric Fondrinier, and Emile Daraï. "Fertility after conservative treatment for borderline ovarian tumors: a French multicenter study." Fertility and sterility 83, no. 2 (2005): 284-290.

Yazbek, J., Lieveke Ameye, Dirk Timmerman, Antonia Carla Testa, Lil Valentin, T. K. Holland, C. Van Holsbeke, and D. Jurkovic. "Use of ultrasound pattern recognition by expert operators to identify borderline ovarian tumors: a study of diagnostic performance and interobserver agreement." Ultrasound in Obstetrics and Gynecology: The Official Journal of the International Society of Ultrasound in Obstetrics and Gynecology 35, no. 1 (2010): 84-88.

Sobiczewski P, Dańska-Bidzińska A, Rzepka J, Kupryjańczyk J, Gujski M, Bidziński M, Michalski W. Evaluation of selected ultrasonographic parameters and marker levels in the preoperative differentiation of borderline ovarian tumors and ovarian cancers. Archives of gynecology and obstetrics. 2012 Dec;286(6):1513-9.

De Souza, Nandita M., Richard O'Neill, G. Angus McIndoe, Roberto Dina, and W. Patrick Soutter. "Borderline tumors of the ovary: CT and MRI features and tumor markers in differentiation from stage I disease." American Journal of Roentgenology 184, no. 3 (2005): 999-1003.

Lee, Eun Joo, See Hyung Kim, Young Hwan Kim, and Hee Jung Lee. "Is CA-125 an additional help to radiologic findings for differentiation borderline ovarian tumor from stage I carcinoma?." Acta Radiologica. 2011; 52, no. 4: 458-462.

Van Calster B, Timmerman D, Bourne T, Testa AC, Van Holsbeke C, Domali E, Jurkovic D, Neven P, Van Huffel S, Valentin L. Discrimination between benign and malignant adnexal masses by specialist ultrasound examination versus serum CA-125. J Natl Cancer Inst. 2007 Nov 21;99(22):1706-14. doi: 10.1093/jnci/djm199. Epub 2007 Nov 13. PMID: 18000221.

Shin JE, Choi HJ, Kim MH, Cho KS. The serum CA-125 concentration data assists in evaluating CT imaging information when used to differentiate borderline ovarian tumor from malignant epithelial ovarian tumors. Korean J Radiol. 2011 Jul-Aug;12(4):456-62. doi: 10.3348/kjr.2011.12.4.456. Epub 2011 Jul 22. PMID: 21852906; PMCID: PMC3150673.

Cormio, G., Loizzi, V., Falagario, M., Scardigno, D., Latorre, D., & Selvaggi, L. E. Borderline Epithelial Tumors of the Ovary. Ovarian Cancer: A Clinical and Translational Update, 2013; 77.

Bent CL, Sahdev A, Rockall AG, Singh N, Sohaib SA, Reznek RH. MRI appearances of borderline ovarian tumors. Clin Radiol 2009; 64:430–438.

Zhao SH, Qiang JW, Zhang GF, Boyko OB, Wang SJ, Cai SQ, et al. MRI appearances of ovarian serous borderline tumor: pathological correlation. J Magn Reson Imaging. 2014;40(1):151–6.

Valentin L, Ameye L, Jurkovic D, Metzger U, Lecuru F, Van Huffel S, Timmerman D. Which extrauterine pelvic masses are difficult to correctly classify as benign or malignant on the basis of ultrasound findings and is there a way of making a correct diagnosis? Ultrasound Obstet Gynecol. 2006; 27:438–444

Park SB, Kim MJ, Lee KH, Ko Y. Ovarian serous surface papillary borderline tumor: characteristic imaging features with clinicopathological correlation. Br J Radiol. 2018;91(1088):20170689.

Morotti M, Menada MV, Gillott DJ, Venturini PL, Ferrero S. The preoperative diagnosis of borderline ovarian tumors: a review of current literature. Archives of gynecology and obstetrics. 2012 Apr;285(4):1103-12.

Li, Yong Ai, Jin Wei Qiang, Feng Hua Ma, Hai Ming Li, and Shu Hui Zhao. "MRI features and score for differentiating borderline from malignant epithelial ovarian tumors." European journal of radiology 98 (2018): 136-142.

Kaga T, Kato H, Hatano Y, Kawaguchi M, Furui T, etal. Can MRI features differentiate ovarian mucinous carcinoma from mucinous borderline tumor. European Journal of Radiology. 2020 Nov 1;132:109281.

Shen-Gunther J, Mannel RS. Ascites as a predictor of ovarian malignancy. Gynecol Oncol. 2002 Oct;87(1):77-83. doi: 10.1006/gyno.2002.6800. PMID: 12468346.

Byun JY, Rha SE, Jung SE, et al. CT and MRI findings of cystadenofibromas of the ovary. Eur Radiol 2004;14(5):798–804. DOI: 10.1007/s00330-

003- 2060-z.
Dubey S, Kaushal A, Pavithra HN."Benign Cystadenofibroma Masquerading Malignant Tumor." The Journal of Medical Sciences (2020): 10.5005/jp-journals-10045-00147
Kawaguchi M, Kato H, Hatano Y, Tomita H, Hara A, Suzui N, Miyazaki T, Furui T, Morishige KI, Matsuo M. MR imaging findings of low-grade serous carcinoma of the ovary: comparison with serous borderline tumor. Japanese journal of radiology. 2020 Aug;38(8):782-9.
Moro F, Zannoni GF, Arciuolo D, Pasciuto T, Amoroso S, Mascilini F, Mainenti S, Scambia G, and Testa AC. "Imaging in gynecological disease (11): clinical and ultrasound features of mucinous ovarian tumors." Ultrasound in Obstetrics & Gynecology 50, no. 2 (2017): 261-270.
Yazbek, J., Raju, K. S., Ben-Nagi, J., Holland, T., Hillaby, K., & Jurkovic, D. Accuracy of ultrasound subjective 'pattern recognition'for the diagnosis of borderline ovarian tumors. Ultrasound in Obstetrics and Gynecology: The Official Journal of the International Society of Ultrasound in Obstetrics and Gynecology, 2007; 29(5), 489-495.
Pascual, M. Angela, Francisco Tresserra, Pedro J. Grases, Ramon Labastida, and Santiago Dexeus. "Borderline cystic tumors of the ovary: gray-scale and color Doppler sonographic findings." Journal of clinical ultrasound. 2002; 30, 2: 76-82.
Geomini PMAJ, Kluivers KB, Moret E, Bremer GL, Kruitwagen RFPM, Mol BWJ (2006) Evaluation of adnexal masses with threedimensional ultrasonography. Obstet Gynecol 108:1167–117
Dogheim OY, Abdel Hamid AM, Barakat MS, Eid M and El Sayed SM. Role of novel magnetic resonance imaging sequences in characterization of ovarian masses, The Egyptian Journal of Radiology and Nuclear Medicine 2014; 45(1): 237-251.
El Ameen, Nadia F., Mohamed G. Eissawy, Laila Adel MS Mohsen, Omnia M. Nada, and Gerges M. Beshreda. "MR diffusion and MR dynamic contrast enhanced sequences in characterization of ovarian tumors." MJMR, Vol. 30, No. 4, 2019.
Thomassin-Naggara I, Toussaint I, Perrot N, Rouzier R, Cuenod CA, Bazot M and Darai E. Characterization of complex adnexal masses: value of adding perfusion- and diffusion-weighted MR imaging to conventional MR imaging. Radiology 2011; 258(3):793–803.
Mohaghegh P and Rockall AG. Imaging Strategy for Early Ovarian Cancer: Characterization of Adnexal Masses with Conventional and Advanced Imaging Techniques. RadioGraphics 2012; 32:1751–1773.
Kierans AS, Bennett GL, Mussi TC, Babb JS, Rusinek H, Melamed J, and Rosenkrantz AB. Characterization of malignancy of adnexal lesions using ADC entropy: comparison with mean ADC and qualitative DWI assessment 2012; 37:164-171.
Nougaret S, Tirumani SH, Addley H, Pandey H, pearls and pitfalls in MRI of gynecologic malignancy with Diffusion-weighted Technique, American Journal of Roentgenology 2013; 200:261-276.
Takeuchi M, Matsuzaki K, Nishitani H. Diffusion-weighted magnetic resonance imaging of ovarian tumors: differentiation of benign and malignant solid components of ovarian masses. Journal of computer assisted tomography. 2010 Mar 1;34(2):173-6.
Denewar FA, Takeuchi M, Urano M, Kamishima Y, Kawai T, Takahashi N, et al. Multiparametric MRI for differentiation of borderline ovarian tumors from stage I malignant epithelial ovarian tumors using multivariate logistic regression analysis. Eur J Radiol. 2017;91:116–23.
Mukuda N, Fujii S, Inoue C, Fukunaga T, Tanabe Y, Itamochi H, et al. Apparent diffusion coefficient (ADC) measurement in ovarian tumor: effect of region-of-interest methods on ADC values and diagnostic ability. J Magn Reson Imaging. 2016;43(3):720–5.